Nonlinear compression of high energy fiber amplifier pulses in air-filled hypocycloid-core Kagome fiber

Florent Guichard,[1,2,*] Achut Giree,[3,4] Yoann Zaouter,[1] Marc Hanna,[2] Guillaume Machinet,[1] Benoît Debord,[5] Frédéric Gérôme,[5,6] Pascal Dupriez,[7] Frédéric Druon,[2] Clemens Hönninger,[1] Eric Mottay,[1] Fetah Benabid,[5,6] and Patrick Georges[2]

[1]Amplitude Systèmes, 11 avenue de Canteranne, Cité de la Photonique, 33600 Pessac, France
[2]Laboratoire Charles Fabry, UMR 8501, Institut d'Optique, CNRS, Univ Paris Sud 11, 2 Av. A. Fresnel, 91127 Palaiseau, France
[3]Amplitude Technologies, 2-4 rue du Bois Chaland CE 2926, 91029 Evry, France
[4]Max Born Institute, Max-Born-Str. 2a, D-12489 Berlin, Germany
[5]GPPMM Group, Xlim Research Institute, CNRS UMR 7252, University of Limoges, France
[6]GLOphotonics S.A.S, Ester Technopole, 1 Avenue d'Ester, 87069 Limoges, France
[7]Alphanov, Optics and Laser Technology Center, Rue François Mitterrand, 33400 Talence, France
[*]florent.guichard@institutoptique.fr

Abstract: We report on the generation of 34 fs and 50 µJ pulses from a high energy fiber amplifier system with nonlinear compression in an air-filled hypocycloid-core Kagome fiber. The unique properties of such fibers allow bridging the gap between solid core fibers-based and hollow capillary-based post-compression setups, thereby operating with pulse energies obtained with current state-of-the-art fiber systems. The overall transmission of the compression setup is over 70%. Together with Yb-doped fiber amplifier technologies, Kagome fibers therefore appear as a promising tool for efficient generation of pulses with durations below 50 fs, energies ranging from 10 to several hundreds of µJ, and high average powers.

OCIS codes: (060.5295) Photonic crystal fibers; (140.3510) Lasers, fiber; (320.5520) Pulse compression; (320.7090) Ultrafast lasers; (320.7110) Ultrafast nonlinear optics.

References

1. Y. Zaouter, J. Boullet, E. Mottay, and E. Cormier, "Transform-limited 100 µJ, 340 MW pulses from a nonlinear-fiber chirped-pulse amplifier using a grating stretcher-compressor," Opt. Lett. **33**(13), 1527–1529 (2008).
2. A. Klenke, S. Hädrich, T. Eidam, J. Rothhardt, M. Kienel, S. Demmler, T. Gottschall, J. Limpert, and A. Tünnermann, "22 GW peak-power fiber chirped-pulse-amplification system," Opt. Lett. **39**(24), 6875–6878 (2014).
3. R. A. Fisher, P. L. Kelley, and T. K. Gustafson, "Subpicosecond pulse generation using the optical Kerr effect," Appl. Phys. Lett. **14**(4), 140 (1969).
4. A. Vernaleken, J. Weitenberg, T. Sartorius, P. Russbueldt, W. Schneider, S. L. Stebbings, M. F. Kling, P. Hommelhoff, H.-D. Hoffmann, R. Poprawe, F. Krausz, T. W. Hänsch, and T. Udem, "Single-pass high-harmonic generation at 20.8 MHz repetition rate," Opt. Lett. **36**(17), 3428–3430 (2011).
5. T. Südmeyer, F. Brunner, E. Innerhofer, R. Paschotta, K. Furusawa, J. C. Baggett, T. M. Monro, D. J. Richardson, and U. Keller, "Nonlinear femtosecond pulse compression at high average power levels by use of a large-mode-area holey fiber," Opt. Lett. **28**(20), 1951–1953 (2003).
6. C. Jocher, T. Eidam, S. Hädrich, J. Limpert, and A. Tünnermann, "Sub 25 fs pulses from solid-core nonlinear compression stage at 250 W of average power," Opt. Lett. **37**(21), 4407–4409 (2012).
7. J. Rothhardt, S. Hädrich, H. Carstens, N. Herrick, S. Demmler, J. Limpert, and A. Tünnermann, "1 MHz repetition rate hollow fiber pulse compression to sub-100-fs duration at 100 W average power," Opt. Lett. **36**(23), 4605–4607 (2011).
8. S. Hädrich, A. Klenke, A. Hoffmann, T. Eidam, T. Gottschall, J. Rothhardt, J. Limpert, and A. Tünnermann, "Nonlinear compression to sub-30-fs, 0.5 mJ pulses at 135 W of average power," Opt. Lett. **38**(19), 3866–3869 (2013).

#231461 - $15.00 USD Received 2 Jan 2015; revised 16 Feb 2015; accepted 19 Feb 2015; published 12 Mar 2015

9. J. Rothhardt, S. Hädrich, A. Klenke, S. Demmler, A. Hoffmann, T. Gotschall, T. Eidam, M. Krebs, J. Limpert, and A. Tünnermann, "53 W average power few-cycle fiber laser system generating soft x rays up to the water window," Opt. Lett. **39**(17), 5224–5227 (2014).
10. M. Nisoli, S. De Silvestri, O. Svelto, R. Szipöcs, K. Ferencz, Ch. Spielmann, S. Sartania, and F. Krausz, "Compression of high-energy laser pulses below 5 fs," Opt. Lett. **22**(8), 522–524 (1997).
11. Y. Y. Wang, N. V. Wheeler, F. Couny, P. J. Roberts, and F. Benabid, "Low loss broadband transmission in hypocycloid-core Kagome hollow-core photonic crystal fiber," Opt. Lett. **36**(5), 669–671 (2011).
12. F. Couny, F. Benabid, P. J. Roberts, P. S. Light, and M. G. Raymer, "Generation and Photonic Guidance of Multi-Octave Optical-Frequency Combs," Science **318**(5853), 1118–1121 (2007).
13. Y. Wang, F. Couny, P. J. Roberts, and F. Benabid, "Low loss broadband transmission in optimized core-shape Kagome hollow-core PCF, "in *Conference on Lasers and Electro-Optics 2010*, OSA Technical Digest Series (CD) (Optical Society of America, 2010), paper p. CPDB4.
14. B. Debord, M. Alharbi, T. Bradley, C. Fourcade-Dutin, Y. Y. Wang, L. Vincetti, F. Gérôme, and F. Benabid, "Hypocycloid-shaped hollow-core photonic crystal fiber Part I: Arc curvature effect on confinement loss," Opt. Express **21**(23), 28597–28608 (2013).
15. B. Debord, M. Alharbi, L. Vincetti, A. Husakou, C. Fourcade-Dutin, C. Hoenninger, E. Mottay, F. Gérôme, and F. Benabid, "Multi-meter fiber-delivery and pulse self-compression of milli-Joule femtosecond laser and fiber-aided laser-micromachining," Opt. Express **22**(9), 10735–10746 (2014).
16. F. Emaury, C. F. Dutin, C. J. Saraceno, M. Trant, O. H. Heckl, Y. Y. Wang, C. Schriber, F. Gérôme, T. Südmeyer, F. Benabid, and U. Keller, "Beam delivery and pulse compression to sub-50 fs of a modelocked thin-disk laser in a gas-filled Kagome-type HC-PCF fiber," Opt. Express **21**(4), 4986–4994 (2013).
17. S. Tzortzakis, L. Bergé, A. Couairon, M. Franco, B. Prade, and A. Mysyrowicz, "Breakup and Fusion of Self-Guided Femtosecond Light Pulses in Air," Phys. Rev. Lett. **86**(24), 5470–5473 (2001).
18. H. Layertec Gmb, *https://www.layertec.de/en/shop/datasheet/101849*, accessed 2/8/2014.
19. M. Nurhuda and E. van Groesen, "Effects of delayed Kerr nonlinearity and ionization on the filamentary ultrashort laser pulses in air," Phys. Rev. E Stat. Nonlin. Soft Matter Phys. **71**(6), 066502 (2005).
20. F. Guichard, Y. Zaouter, M. Hanna, F. Morin, C. Hönninger, E. Mottay, F. Druon, and P. Georges, "Energy scaling of a nonlinear compression setup using passive coherent combining," Opt. Lett. **38**(21), 4437–4440 (2013).
21. A. Klenke, S. Hädrich, M. Kienel, T. Eidam, J. Limpert, and A. Tünnermann, "Coherent combination of spectrally broadened femtosecond pulses for nonlinear compression," Opt. Lett. **39**(12), 3520–3522 (2014).
22. F. Emaury, C. J. Saraceno, B. Debord, D. Ghosh, A. Diebold, F. Gèrôme, T. Südmeyer, F. Benabid, and U. Keller, "Efficient spectral broadening in the 100-W average power regime using gas-filled kagome HC-PCF and pulse compression," Opt. Lett. **39**(24), 6843–6846 (2014).

1. Introduction

The generation of high-energy and ultrashort pulses is usually limited by the available gain bandwidth of ultrashort amplifiers. In the case of Ytterbium-doped fiber amplifiers, the typical available bandwidth is of the order of 40 nm, limiting the pulse duration of high-energy fiber chirped-pulse amplifiers (FCPA) around 300 fs [1] or close to 200 fs with phase shaping [2]. In order to decrease this pulsewidth well below 100 fs, e. g. to drive high-field physics experiments, or match material processing requirements, nonlinear compression techniques are required. These techniques consist in nonlinearly broadening the spectrum of incident laser pulses mainly via self-phase modulation [3]. Suppression of the induced spectral chirp produced by the nonlinear interaction in the medium with appropriate dispersive elements then leads to pulse shortening. The nonlinear interaction is usually carried out in a waveguide to allow a strong confinement of the electric field over a long distance while maintaining a good spatial profile of the output beam. For the range of parameters usually available from state of the art FCPA, nonlinear compression is either performed in a silica solid-core fiber with energy limited by the self-focusing threshold (up to the μJ level [4–6]) or in gas-filled hollow core capillaries for higher input energy (from 200 μJ up to several mJ [7–9]), following a technique routinely used for Titanium-doped Sapphire (Ti:Sa) CPA systems [10]. In the latter case, the low output energy ($10< E < 500$ μJ) and the long pulse length (typically from 300 fs up to 1ps) of FCPAs compared to bulk Ti:Sa systems necessitates longer interaction lengths, higher gas pressures, and lower diameters. This significantly increases the complexity and decreases the transmission of capillary-based nonlinear compression setups to 50% or less [7–9]. There is therefore a clear lack of waveguide that could support efficient spectral broadening in a straightforward arrangement

#231461 - $15.00 USD Received 2 Jan 2015; revised 16 Feb 2015; accepted 19 Feb 2015; published 12 Mar 2015

of high repetition rate sources with energy levels typically ranging from tens to hundreds of μJ.

The recent development of hypocycloid-core Kagome (HCK) fibers [11] is a promising way to bridge this gap of energy range for nonlinear compression setups between solid core fibers and gas-filled capillaries. Indeed, in such structure the solid silica core is replaced by a hollow-core satisfying the guiding condition through inhibited coupling (IC) [12] allowing optical-guidance for large core diameters over large spectral range. Such properties stem from the fact that, unlike photonic bandgap hollow-core fibers, the guiding mechanism does not rely on the total absence of cladding modes (i.e. bandgap) but, akin to quasi-bound state in a continuum, based on a strong coupling inhibition with the cladding modes. This IC mechanism was further enhanced with the seminal introduction of a hypocycloid-core shape [11, 13], characterized by negative curvature silica bridges along the core contour, and allows an important decrease of the overlap integral between the intense guided mode and the surrounding silica structure closed to the ppm level by sufficiently increasing the silica bridge negative curvature [14]. This ensures low propagation losses and dramatically reduced fiber damage threshold allowing mJ pulse energy delivery with intensities nearing petawatts per square centimeter [15]. A recent experimental effort to use such fibers in a standard nonlinear compression setup has allowed for the demonstration operation at a moderate energy level of 1.1 μJ [16]. This experiment has been performed with noble gas-filled fibers, which imply an increased complexity compared to air-filled structure at atmospheric pressure. Another recent report focuses on self-compression of 500 μJ pulses in the anomalous dispersion regime [15]. In this case, the compression relies on higher-order soliton propagation regimes, making the system less controllable than a standard compression setup.

In this article, we focus on the energy limitations of a post-compression setup based on a short length of state-of-the-art hypocycloid Kagome fiber filled at atmospheric pressure with air. We report on nonlinear compression of 330 fs 70 μJ input pulses down to 34 fs and 50 μJ at a repetition rate of 50 kHz, corresponding to an average power of 2.5 W. This result is achieved by exploiting self-phase modulation occurring in a 1.2 m long air-filled hypocycloid-core Kagome fiber, with high overall efficiency of more than 70%. To our knowledge this is the first post-compression experiment done in a waveguide with an input energy in the range 10 – 200 μJ at high repetition rate. The unique combination of waveguide properties and geometrical dimensions of these fibers make them the ideal structure to achieve nonlinear post-compression at the output of high-energy FCPAs with excellent overall transmission efficiency. The air-filled configuration allows a simple, compact and robust setup.

2. Hypocycloid-core Kagome fiber

The fiber structure used in our experiment is arranged in a 7-cell core and 3-ring cladding geometry. The fiber outer diameter is 350 μm and the core exhibits a diameter of 56 μm and of 72 μm for the inner and outer circumscribing cups respectively. The resulting mode-field diameter (MFD) is ~40 μm [*see* Fig. 1(a)]. The fiber parameters are designed for optimal operation in the near infrared region. The linear propagation properties of the fiber are plotted in Fig. 1(b), namely experimentally measured propagation losses (gray curve) and group velocity dispersion (GVD, red curve) obtained from finite-elements numerical simulations. The Kagome lattice exhibits in its first-order transmission band a 210 nm-broad and low loss guiding wavelength range in the near infrared. Propagation losses are kept below 200 $dB.km^{-1}$ from 990 nm to 1200 nm with a minimum of 20 $dB.km^{-1}$. The simulated GVD of the fiber is low and normal at 1030 nm with a value $\beta_2 = +5.6\times10^{-4}$ $ps^2.m^{-1}$. This low value is advantageous in nonlinear compression setups since it limits temporal pulse spreading and therefore maintains a high-peak power along propagation in the fiber. Indeed, in our case with

#231461 - $15.00 USD Received 2 Jan 2015; revised 16 Feb 2015; accepted 19 Feb 2015; published 12 Mar 2015

an input pulse duration $T_0 =$ 330 fs the corresponding dispersion length is $L_D = \frac{T_0^2}{|\beta_2|} = 194\,m$, a value well above the Kagome fiber length. Operating near the zero-dispersion wavelength might not appear optimal due to the generation of spectral content in the anomalous dispersion regime. Indeed, in the case of waveguide exhibiting negative dispersion and SPM, soliton compression effects make the compression system much less controllable. Operating near the zero GVD point makes third-order dispersion effects more important, leading to an asymmetric oscillatory trailing edge. We have checked using numerical simulations that in our experimental conditions, this does not significantly degrade the output pulse quality. In our case this effect slightly decreases the output pulse quality, but not to a dramatic extent. Furthermore, the dispersion properties could in the future be engineered to push the zero dispersion-wavelength further towards the long wavelengths side.

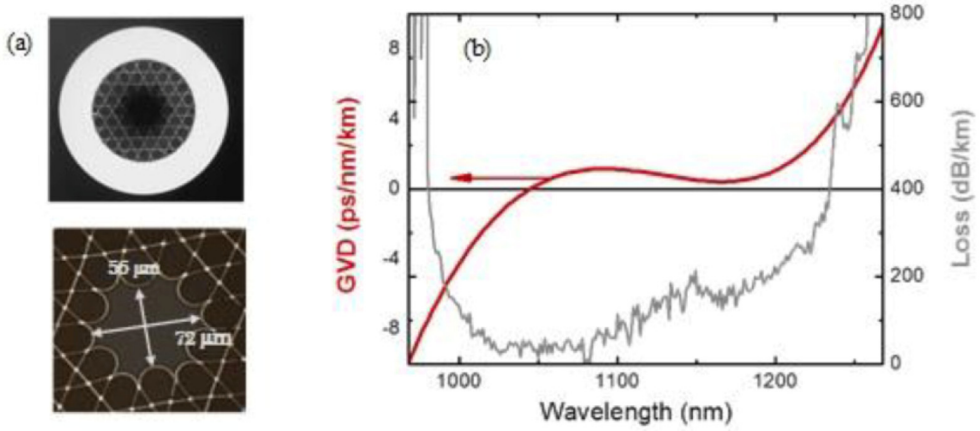

Fig. 1. (a) Image of the whole fiber and zoom on the hypocycloid-core shape. (b) Linear propagation properties, group velocity dispersion (red curve) and propagation losses (gray curve) of the hypocycloid-core Kagome fiber used in our experiment.

3. Experimental setup and results

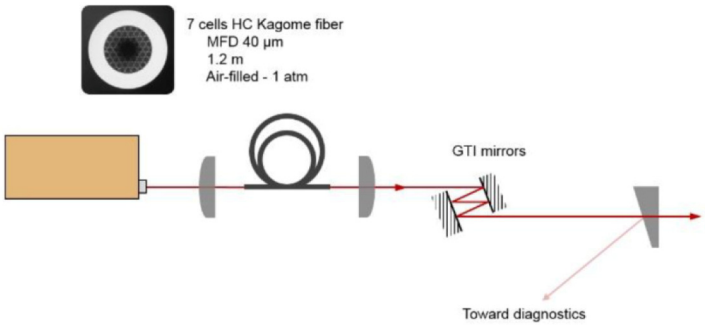

Fig. 2. Experimental IC hypocycloid-core Kagome fiber based nonlinear compression setup. Insert: transverse profile of the fiber.

The experimental setup is depicted in Fig. 2, starting with a fiber-based laser source able to deliver 330 fs transform-limited pulses with an output energy of up to 150 µJ at a repetition rate of 50 kHz. This beam is coupled to the previously detailed 1.2 m-long HCK fiber, mounted in V grooves, and coiled with a radius of curvature of approximately 15 cm. The fiber is operated without any pressure regulation system, and is therefore filled with air at

#231461 - $15.00 USD Received 2 Jan 2015; revised 16 Feb 2015; accepted 19 Feb 2015; published 12 Mar 2015

atmospheric pressure. Taking into account the laser parameters and assuming a nonlinear refractive index for the air of $n_2 \sim 3.2\times10^{-23}$ $m^2.W^{-1}$ [17], numerical simulations reveal that air imparts sufficient SPM to significantly broaden the optical spectrum and achieve large compression ratios. Moreover, the nonlinear response of air contains a delayed part, with a time constant of the order of 70 fs and a relative magnitude of the same order than the instantaneous part. In our experimental condition, simulations indicate that this Raman response translates into a slight asymmetry of the broadened spectrum towards the long wavelength part, and does not prevent proper compression. This considerably simplifies the overall experimental setup, avoiding the use of expensive noble gas and complex high-pressure systems. The output beam is collimated and spectrally broadened pulses are compressed using several bounces on −100 fs^2 Gires-Tournois Interferometer (GTI) mirrors (Layertec GmbH) [18]. This compressor provides a high transmission efficiency. Finally, a wedged window is used to sample the beam for output spatial and temporal characterizations.

The input energy in the HCK fiber is gradually increased and the negative dispersion introduced by the compressor simultaneously optimized to provide the shortest pulses with best temporal quality. Best results are obtained for an output energy of 50 µJ and total compressor GVD of −2100 fs^2. In this configuration the compressor efficiency is 93%. Above this energy level the spectral broadening extends beyond the reflection band of the dielectric mirrors used to steer the beam therefor preventing further compression. The overall power transmission of 71% can be decomposed in 81% fiber coupling efficiency, 94% fiber transmission, and 93% compressor transmission. At the output of the fiber, the degree of linear polarization is >90%.

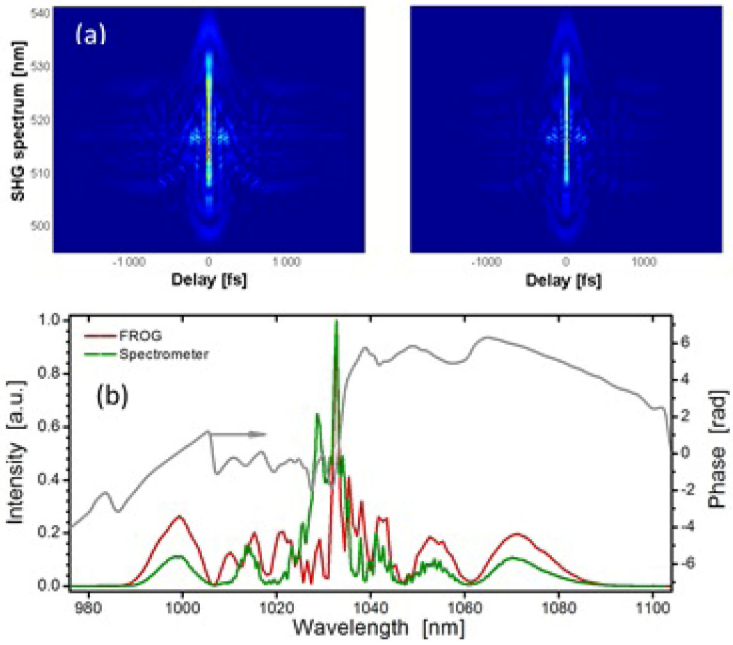

Fig. 3. (a) Measured (left) and retrieved (right) FROG trace at 50 µJ. (b) Retrieved output spectrum, gray curve corresponds to the retrieved spectral phase.

Temporal characterizations of the output pulse at 50 µJ of energy are carried out with a second harmonic generation frequency-resolved optical gating (SHG-FROG) device together with independent spectrum measurement. Results are plotted in Fig. 3. The electric field reconstruction is carried out on a 1024x1024 grid [*see* Fig. 3(a)] and converges to a FROG

#231461 - $15.00 USD Received 2 Jan 2015; revised 16 Feb 2015; accepted 19 Feb 2015; published 12 Mar 2015

error of 70 × 10^{-4}. The validity of the FROG measurement is checked by comparison with independent spectral measurements shown in Fig. 3(b) revealing that the measured spectrum is in qualitative agreement with the retrieved data, except for the central peak located at 1030 nm. The spectral width measured at −10 dB is 90 nm. The spectral phase is also plotted in Fig. 3(b) (gray curve) and shows non-negligible remaining structures. In particular, the central spectral peak exhibits a large spectral phase slope, corresponding to a group delay in the time domain. We verified that this peak corresponds to the broad post-pulse observed in the time domain 700 fs away from the main peak. Our current interpretation is that it is due to an initial pedestal of the FCPA and/or to residual coupling to a higher order mode of the structure propagating at a different group velocity. The latter interpretation can also explain that the peak magnitude is not consistently measured by the characterization equipment, since it is carried by a different spatial mode. Other residual phase terms are of much lower magnitude, and are mainly dominated by uncompensated high-order terms arising from the GTI mirrors. In the time domain, the retrieved 34 fs FWHM temporal profile is shown in Fig. 3(c). The energy carried by the main pulse in the time domain is 65% of the total energy content. The Fourier-transform limited duration is 30 fs, indicating that the residual spectral phase has a modest impact on final pulse duration. Despite the pedestal, with an output energy of 50 μJ, the retrieved pulse profile has a peak power of 730 MW, to be compared to 1100 MW if the Fourier transform-limited pulse is considered. With an input peak-power of 200 MW, these results correspond to a peak-power enhancement factor of 3.65 together with a 10-fold decrease of the temporal duration.

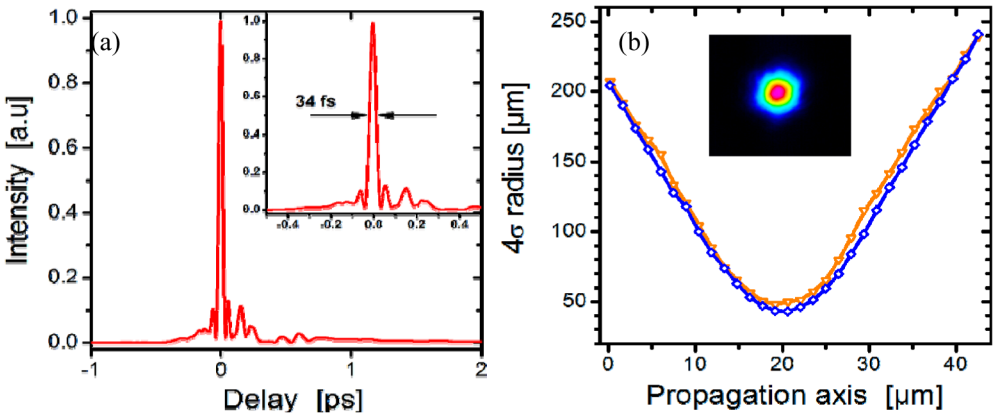

Fig. 4. (a) Retrieved 34 fs temporal profile, with associated peak-power. Insert: Emphasis on the time interval [-500 500] fs. (b) Beam caustic along two orthogonal axis. Insert: Typical far-field beam profile at 50 μJ of output energy.

The spatial quality of the output beam is good owing to the guiding properties of the HCK fiber. The M^2 values at the output of the FCPA are 1.2 in both transverse directions. At the output of the HCK fiber M^2 values are 1.3 and 1.45, as shown in Fig. 4(b). The far-field beam profile exhibits a nearly Gaussian-shape [*see* insert in Fig. 4(b)]. We believe that these values could be decreased with better coupling efficiency to reduce the residual higher order guided modes.

#231461 - $15.00 USD Received 2 Jan 2015; revised 16 Feb 2015; accepted 19 Feb 2015; published 12 Mar 2015

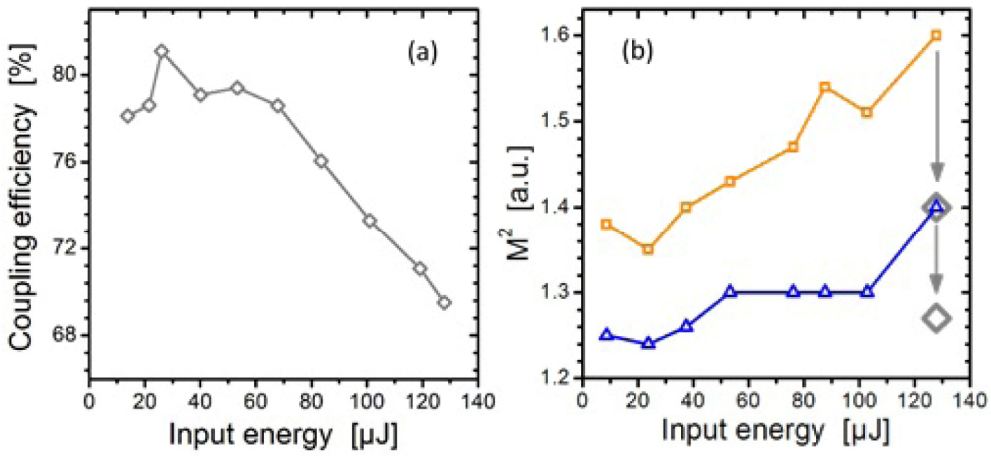

Fig. 5. (a) Fiber transmission efficiency with respect to the input energy. (b) M-squared evolution along two orthogonal axis with the input energy, gray arrows and diamonds indicate the displacement and the new position of M^2 values after peak-power reduction.

We also investigate the limitations of this setup in terms of pulse energy. To do so, the fiber power transmission and the M^2 of the compressed beam are recorded as a function of input pulse energy. Results are plotted in Fig. 5 and show a drop of the transmission efficiency correlated with a degradation of the output spatial quality. The transmission efficiency remains at 74% for input energies below 70 µJ and linearly decreases for higher energies. Correspondingly, M^2 values increase from a minimal value of 1.25 and 1.36 to reach 1.4 and 1.6 at 130 µJ input energy. This behavior is attributed to the onset of significant ionization of air near the fiber input, which degrades the coupling efficiency to the fundamental core-mode, and thus exciting higher order modes. Indeed, for an input energy of 60 µJ, the corresponding peak intensity is already of the order of 10^{13} W.cm^{-2}, a value at which air-ionization becomes important [19]. Comparatively, the critical power for self-focusing in air is of the order of ~10 GW, which is well above the peak powers in our setup, therefore playing a negligible role. The efficiency drop and spatial beam quality degradation can thus be understood as a consequence of significant ionization that couples part of the propagating light outside of the fundamental mode through plasma defocusing effect as previously observed in [19]. This non-negligible power coupled to the fiber microstructure and high-order modes is partially filtered after propagation in the 1.2 m long Kagome fiber, resulting in a transmission efficiency drop. The output beam also exhibits a non-filtered high-order mode residual component that degrades the spatial quality. To confirm the intensity dependence of these effects, we observe a clear spatial quality and transmission efficiency improvement when the input pulse peak-power is reduced at constant pulse energy by detuning the FCPA compressor unit (*see* gray arrows and diamonds in Fig. 4(b)).

6. Conclusion

In summary, we achieve nonlinear compression of 330 fs 70 µJ pulses generated by a FCPA system down to 34 fs with 50 µJ energy, corresponding to a transmission efficiency of 70%. These results rely on the outstanding properties of a HCK fiber having a core diameters larger than 40 µm filled with air at atmospheric pressure. The setup is currently limited by the onset of ionization in the air-filled core that decreases the transmission efficiency and the output spatial quality. However, this limit can readily be pushed toward to 200 µJ by using larger core fiber with 80 µm MFD [15] and beyond using coherent combining techniques such as the divided-pulse nonlinear-compression concepts [20, 21], making HCK fibers an ideal compression tool for high repetition rate high-energy fiber amplifier systems. The authors

#231461 - $15.00 USD Received 2 Jan 2015; revised 16 Feb 2015; accepted 19 Feb 2015; published 12 Mar 2015

believe that air-filled HCK fibers are of considerable interest to bridge the gap between solid-core fibers-based and hollow capillaries-based post compression setups, thereby performing nonlinear compression of femtosecond pulses with energies lying in the 1 μJ – 500 μJ range with simple and compact setups together with high efficiencies. Beyond this energy range, gas-filled capillary can be readily used. Although the average power level in this work is low (2.5 W), a recent demonstration of post-compression in HCK fibers at 100 W level [22], although done with longer pulses and at a lower energy level, shows the scaling potential of this setup. Indeed, this average power level is easily and currently achieved by standard FCPA sources. However, in that case careful attention must be paid to properly hold the fiber and avoid beam pointing drifts induced at high average power.

Acknowledgments

The authors acknowledge financial support from "Agence Nationale de la Recherche (ANR)" (grants PHOTOSYNTH and Σ_LIM Labex Chaire, Astrid UV-Factor) and by "la région Limousin".

#231461 - $15.00 USD Received 2 Jan 2015; revised 16 Feb 2015; accepted 19 Feb 2015; published 12 Mar 2015